Aromatic-Based Design of Highly Active and Noncalcemic Vitamin D Receptor Agonists

Pranjal Gogoi, Samuel Seoane, Rita Sigüeiro, Thierry Guiberteau, Miguel Maestro, Román Pérez-Fernández, Natacha Rochel, Antonio Mouriño

Aromatic-Based Design of Highly Active and Noncalcemic Vitamin D Receptor Agonists

Pranjal Gogoi,[†#+] Samuel Seoane,[‡#] Rita Sigüeiro,[†§#] Thierry Guiberteau,[¤] Miguel A. Maestro,[¶] Román Pérez-Fernández,[‡] Natacha Rochel,[§]* Antonio Mouriño.[†]**

[†]Department of Organic Chemistry, Research Laboratory Ignacio Ribas, University of Santiago de Compostela, Avda. das Ciencias s/n, 15782 Santiago de Compostela, Spain

[‡]Department of Physiology–Center for Research in Molecular Medicine and Chronic Diseases (CIMUS), University of Santiago de Compostela, Avda. Barcelona s/n, 15706 Santiago de Compostela, Spain

[§]Department of Integrative Structural Biology, IGBMC - Université de Strasbourg, CNRS UMR 7104, INSERM U1258, 67400 Illkirch, France

[¤]Laboratoire ICube - Université de Strasbourg, CNRS UMR 7357, 67000 Strasbourg, France

[¶]Department of Chemistry-CICA, University of A Coruña, Campus da Zapateira s/n, 15071 A Coruña, Spain

[+]Current address: Chemical Science and Technology Division, CSIR-NEIST, Jorhat, Assam, India

KEYWORDS: active vitamin D analog; calcemia; antiproliferation; crystal structure

ABSTRACT

We report the design, synthesis, biological evaluation and structural analysis of a new class of vitamin D analogs that possess an aromatic *m*-phenylene **D**-ring and an alkyl chain replacing the **C**-ring. A key feature of the synthetic strategy is a stereoselective Pd-catalyzed construction of the triene system in aqueous medium that allows the rapid preparation of small amounts of VDR ligands for biological screening. Analogs with the shorter (**2a**) and longer (**2d**, **2e**) side chains attached to the triene system have no calcemic activity. Compound **2a** binds to VDR with the same order of magnitude than calcipotriol and oxacalcitriol. It also reduces proliferation in normal and tumor cells similarly to the natural hormone 1α,25-dihydroxyvitamin D_3, calcipotriol and oxacalcitriol, suggesting preclinical studies related to hyperproliferative disorders such as psoriasis and cancer.

INTRODUCTION

Increasing synthetic efforts have been directed toward the development of noncalcemic analogs of the natural hormone 1α,25-dihydroxyvitamin D_3 (1,25D, calcitriol, **1**, Fig. 1a) for treatment of specific disorders, but only a few of them have found clinical applications.[1,2] Among these, calcipotriol[3] and oxacalcitriol (OCT),[4] two 1,25D-analogs modified at the side chain, have been successfully used for topical treatment of psoriasis, because they are rapidly metabolized before exerting calcemic effects.[5] Various classic synthetic 1,25D analogs have been shown to have anti-tumor activities.[2] Highly active 1,25D-analogs that exert less calcemic activity than the natural hormone by a non rapid metabolism and unknown mechanism have also been developed. The most notable structural features of these compounds include lack of the 19-methylene group,[6] unsaturation at the side chain or **D**-ring,[7,8] 14-epi-configuration,[9,10] 3-epi-configuration,[11] short nonhydroxylated side chains,[12] and carboranic side chains.[13] **CD**-carboranic and aromatic VDR modulators have also been reported.[14,15]

Recently we described a flexible and efficient convergent synthetic approach for the preparation of vitamin D analogs.[16] This synthesis has been used to access the natural hormone 1,25D[17] and a variety of vitamin D analogs modified at the side-chain,[13] triene system,[18] **C**-ring,[19] and **A**-ring,[11,20] that were required to establish structure-function relationships for the development of active ligands of the VDR with potential therapeutic value. Biological studies on analogs with modified **C**/**D** region that comprise **C**-ring analogs lacking the **D**-ring,[21,22] **D**-ring analogs lacking the **C**-ring[23,24] and six-membered **D**-ring analogs,[25,26] have demonstrated that the native bicyclic **CD**-core is not required for biological activity and its alteration might lower the calcemic activity.[27]

In a search for vitamin D analogs that are highly active in the circulation, but with low or negligible calcemic effects, we describe a modification of the reported synthetic approach for rapid and economic access to novel vitamin D analogs **2** (Fig. 1a) and disclose their structures and their biological activities with respect to cell differentiation-proliferation, transactivation and secondary calcemic effects. This novel class of analogs lack the **C**-ring and the **D**-ring is replaced by an aromatic ring, which offers flexibility for further chemical functionalization. Some of these analogs are highly active and noncalcemic in comparison to the natural hormone 1,25D. X-ray crystallographic analysis of VDR complexes with analogs **2** revealed their binding mode.

<FIGURE 1>

RESULTS and DISCUSSION

Aromatic-based design of 1,25D analogs. We previously described the successful structure-based design of highly active and superagonist ligands for the VDR.[18-20] We found that these ligands bind significantly *in silico* to VDR and adopt an elongate conformation similar to that of the natural hormone with the hydroxyl groups interacting through the same hydrogen bonds.[18,19,28] These compounds bind to VDR LBD more efficiently than their corresponding derivatives with shorter hydroxylated side chain. On the basis that alteration of the **CD**-rings lowers the calcemic activity,[27] we designed the five novel 1,25D analogs **2** by *docking* studies into the crystal structure of the hVDR ligand binding domain (LBD)-1,25D complex,[29] to investigate whether the lack of the **C**-ring and the presence of a *m*-phenylene ring replacing the **D**-ring of the natural hormone could serve for the development of potent analogs with improved pharmacological properties, in particular, without the undesired calcemic action. We reasoned

that the aromatic ring might alter the natural ligand-VDR interactions, thus inducing selective properties. In addition, the aromatic unit allows flexibility to access to a large number of aromatic-substituted analogs.

Docking studies were carried out into the hVDR LBD-1,25D crystal complex[29] using the GOLD program (Table S1). In all cases, the **A**-ring and the triene system of the new vitamin D ligands adopt similar positions in comparison with the natural hormone and the **A**-ring-hydroxyl groups form hydrogen bonds with the same amino acid residues (Fig. 1b and Fig. S1). The alkyl chains attached to C8 of the triene system adopt different elongated conformations that interact strongly with the protein residues Trp286 and Tyr295. Side-chain length increasing generates additional interactions with other LBP residues such as Val300. To accommodate the C8-alkyl chains, substantial differences are observed in the conformations adopted by the aromatic rings and the main side chain. In ligands **2a**, **2b** and **2c**, where the C8-alkyl chains are shorter, the aromatic rings show a parallel orientation with respect to Trp286 and the corresponding hydroxylated side chains adopt extended conformations, where the hydroxyl groups interact optimally by hydrogen bonding with His305 and His397. The aromatic unit of ligands **2d** and **2e**, which is attached to the longest C8-alkyl chains, adopts a perpendicular position with respect to Trp286, and the hydroxyl group of the side-chain does not interact with His397 by hydrogen bonding.

Synthesis of compounds 2. The synthetic route to target analogs **2** is described in Scheme 1, and starts with commercially available 3-bromobenzaldehyde (**3**), which was converted to the key alkyne **7** in 66% overall yield over 4 steps. The aldehyde **3** was coupled with freshly prepared organozinc reagent **4**[30] in the presence of catalytic amounts of tris(dibenzylidene-acetone)dipalladium(0) and tri-*tert*-butylphosphine in tetrahydrofuran to provide the ester **5** in

good yield. Chain-extension on **5** by the method of Corey-Fuchs[31] utilizing the ylide prepared from zinc, triphenylphosphine and carbon tetrabromide in dichloromethane, gave the vinyl dibromide **6**, which was treated with methyllithium in tetrahydrofuran to generate **7** with both the tertiary hydroxyl and the alkyne functionalities in good yield. Protection of the tertiary hydroxyl group of **7** with triethylsilyltrifluoromethanesulfonate and triethylamine in dichloromethane afforded alkyne **8**. This four-step synthetic strategy allows flexibility for variations at the side chain and aromatic ring. Next goal was the introduction of the five different alkyl groups corresponding to target analogs **2a**-**e**. This was accomplished in good yield by exposure of **8** to the cuprate generated from the alkylmagnesium bromide, copper(I) iodide and lithium chloride in tetrahydrofuran followed by trapping of the resulting alkenyl copper intermediate with trimethylsilyl chloride in hexamethylphosphoramide. The resulting alkenylsilanes **9a**-**e** were then treated with *N*-iodosuccinimide in dichloromethane to afford stereoselectively the corresponding iodides **10a**-**e** in good yield, which were converted to the desired upper boronates **11a**-**e** by Miyaura's modified method[16,32] utilizing bis(pinacolato)diboron and potasium acetate in the presence of catalytic [1,1'-bis(diphenylphosphino)ferrocene]dichloropalladium(II) in dimethylsulfoxide. With the upper fragment in hand, the stage was set for the final convergent formation of the triene system. Pd-catalyzed ring-closure of the enol triflate **12**[16] (1.1 equiv) and a subsequent Suzuki-Miyaura reaction with boronate **11a-e** (1 equiv) in aqueous medium provided,[16] after deprotection, the desired vitamin D analogs **2a-e** (15-37% overall yield from 3-bromobenzaldehyde, 8 steps).

<SCHEME 1>

Functional activity of compounds 2a-e. It is noteworthy that all *des*-**C**-analogs bind significantly to VDR despite the fact that the natural **CD**-ring is replaced by a linear short side-chain attached to C8 and a *m*-disubstituted benzene ring (Table 1; Fig. S2). These interesting results prompted us to study their biological activity. As in case of 1,25D, all compounds strongly induce differentiation in human keratinocyte cells and increase p21, p27 and p53 protein expression, well-known 1,25D target genes (Table 1; Fig. 2a-b). The new ligands show similar anti-proliferative activity in both bi- and three-dimensional analyses than 1,25D in human normal keratinocytes and breast, prostate, and ovarian cancer cell lines (Table 1; Fig. S3a-f), where **2a,** with shortest chain at C8, is the most active. The *CYP24A1* (24-hydroxylase)-transcriptional activity induced by all compounds correlates with VDR affinity, with **2a** being the most potent one, as compared to 1,25D (Table 1; Fig S4a). These results confirm that the natural **CD**-ring is not required for genomic activity. Notably, in comparison with vehicle-treated mice, none of compounds **2a-e** induce hypercalcemia (Table 1; Fig S4b). Furthermore, high doses of compound **2a** did not increase calcium levels in mice sera (Fig. 3a).

<Table 1>

<Figure 2>

Numerous studies have associated 1,25D with anti-tumoral properties.[33-35] VDR is present in breast cancer cells,[36] and a recent study has shown that VDR expression should be considered for breast cancer treatment.[37] However, hypercalcemia is an undesirable side effect of the natural hormone when used at pharmacological doses.[38] The remarkable lack of calcemic activity of compound **2a**, together with its significant VDR binding and transcriptional activity led us to study its antitumor properties. Severe combined immunodeficiency (SCID) mice injected with

the highly aggressive human breast cancer MDA-MB-231 cell line and treated with compound **2a** significantly reduced tumor growth as compared controls (Fig. 3b-c). Notably, a significant increase in overall survival of **2a** treated-mice without signs of toxicity in the liver and kidney as well as no significant weight loss was also observed (Fig. 3d; Fig. S5a-b). To further study the therapeutic relevance of compound **2a** on the tumorigenesis process, we focus on its effects on cancer stem cells. The role of cancer stem cells in cancer initiation, progression, drug resistance, and relapse[39] is well known. As shown in Fig. 3e-g, a significant decrease in both growth and number of mammospheres was observed after treatment of cancer stem cells (CSC)-like with 100 nM of **2a** as compared to control. Altogether, our data indicate that compound **2a** acts on both cancer cells and cancer stem cells, suggesting that it could be a therapeutic option in breast cancer.

<Figure 3>

Structural features of VDR interaction with compounds 2. The docking data were substantially corroborated by the crystal structures of **2a-2e** bound to the LBD of zebrafish-VDR [(zVDR) LBD] in the presence of SRC-2 coactivator peptide, solved at a resolution of 2.5 Å, 2.7 Å, 2.6 Å, 2.3 Å and 2.75 Å for zVDR-**2a**, -**2b**, -**2c**, -**2d** and -**2e** complexes, respectively (see supporting information and Table S2 for details). All complexes display the canonical agonist conformation of previously reported structures of VDR bound to agonist ligands with helix H12 folded in the agonistic position.[40,41] The ligands are buried in the predominantly hydrophobic pocket and adopt the same orientation as 1,25D (Fig. 4). The alkyl chains attached to C8 of the triene system and the aromatic ring occupy the space filled by the **CD**-rings of the natural 1,25D ligand. Some flexibility of the terminal methyl group of the alkyl chain was observed for most of

the ligands as indicated by the weak density of the corresponding atoms (Fig. S6). A minor discrepancy between modeling and X-ray data is observed for the conformation of the aromatic ring that is identical and parallel to zTrp314 (hTrp286 in docking) in all crystallographic complexes (Fig. 4a). Indeed, the VDR LBP accommodates the different variants of the C8-alkyl central chain through different conformations of the C8-alkyl and aromatic terminal side chains, together with rearrangement of the protein. The three hydroxyl groups of the compounds form H-bonds with a pair of residues for each OH group, similarly to 1,25D (Fig. 4b-f).

The main differences in the interactions of the VDR-**2a-e** complexes compared to the VDR-1,25D complex are observed in the region of the central part (aromatic moiety and C8-alkyl chain) and terminal aliphatic side chain (Fig. 5 and Fig. S7). Interestingly, analogs **2** form tighter interactions with zIle299(hIle268), a specific interaction already observed for some low-calcemic analog.[42] zTrp314 (hTrp286) does not interact with the aromatic moiety of all compounds, but interacts with the C8-alkyl chains. Increasing the length of the C8-alkyl side chain in **2e** leads to the formation of additional interactions as with zMet254 (hMet226) and zVal328 (hVal300) (Fig. 5). However, these additional contacts of the heptyl-chain of **2e** induce a different positioning of the terminal aliphatic side chain and reorientation of some nearby amino acids to maintain interactions. In all complexes, the terminal aliphatic side chains form similar interactions and notably a stronger contact with zPhe448 (hPhe422) in H12 compared to 1,25D. In comparison to bis and tri-aromatic derivatives,[43] the analogs **2** better mimic the conformation of 1,25D and maintain the hydrophobic interaction of 1,25D.

Overall the crystal structures of VDR complexes reveal that analogs **2** form similar interactions as 1,25D, stabilizing the agonistic conformation of VDR.

<Figure 4>

CONCLUSION

This paper reports a series of new analogs which possess a *m*-phenylene **D**-ring and an alkyl chain replacing the **C**-ring. These analogs are clearly no calcemic, but are as active as the nature hormone 1,25D. Indeed, hybrid analogs with the shorter (**2a**) and longer (**2d, 2e**) side chains attached to the triene system have no calcemic activity. The compounds are similarly accommodated by the VDR LBD as 1,25D. The molecular basis for their transcriptional activity is the conservation of the hydrogen binding network and hydrophobic interactions of the natural ligand. While some specific interactions are observed, the relationship among the differential interactions mediated by the ligands compared to 1,25D and non-calcemic activities of the ligands remains to be elucidated. Compound **2a** reduces proliferation in normal and tumor cells similarly to the natural hormone without increasing serum calcium levels. We tested its *in vivo* efficacy in a xenograft model of breast cancer. In the aggressive MDA-MB-231 cells implanted in SCID mice, compound **2a** had high efficacy for tumor growth inhibition and overall survival.

In summary, this study provides important structure-activity relationship information on novel aromatic-based vitamin D analogs. Their properties, combined with the low calcemic actions, make these analogs promising agents for clinical treatment of hyperproliferative disorders including cancer.

EXPERIMENTAL SECTION

Docking procedure. The receptor and the ligands were used as MOL2 files. Energy minimization was not performed on the protein. Compounds **2a-e** were built using the Builder module of the InsightII molecular modeling program[44] and the crystal structure of 1,25D, obtained from the complex of 1,25D-hVDR LBD (protein data bank code: 1DB1).[29] The initial conformation of the ligand was energy-minimized using the Discover program and cvff forcefield (5000-step, steepest descent, in vacuum at 300 K).[45] Finally, docking studies to predict the affinity of the ligands for the VDR were carried out using the GOLD program (version Suite 5.2). A modified crystal structure (addition of hydrogen, reconstituted gaps and corrected His tautomers) of the complex between 1,25D-hVDR LBD was chosen as protein. The Ligand Binding Pocket of the LBD was defined as Binding Site with the automatic active-site detection on, and the radius was set to 10 Å. Ligands were docked in 25 independent genetic algorithm (GA) runs, for each of which a maximum of 125000 GA operations were performed on a single population of 100 individuals. Operator weights for crossover, mutation, and migration in the entry box were used as default parameters (95, 95, and 10, respectively), as well as the hydrogen bonding (4.0 Å) and van der Waals (2.5 Å) parameters. The "flip ring corners" flag was switched off, while all the other flags were on. CHEMPLP was used as a scoring function and GoldScore as a re-scoring function. The best three solutions were obtained with an associated score. The values obtained are shown in the Table S1. The punctuations were compared with those obtained for 1,25D. In all cases, the fitness scores for the new ligands were lower than those obtained for 1,25D.

Cell Culture. Human breast adenocarcinoma MCF-7 and MDA-MB-231 cells, human prostate adenocarcinoma PC3 cells, human ovary adenocarcinoma SKOV-3 cells, and human

keratinocytes HaCaT cells were obtained from ATCC-LGC (Barcelona, Spain). Cells were tested and authenticated according to microscopic morphology, growth curve analysis, and mycoplasma detection according to the ECACC cell line verification test recommendations. Cells were grown in DMEM media supplemented with 10% FBS, 100 U/mL penicillin, 100 U/mL streptomycin, and 2 mM L-glutamine (all from Invitrogen, Paisley, UK), in air-CO_2 (95:5) atmosphere a 37 °C. Confluent cells were washed twice with PBS and harvested by a brief incubation with trypsin−EDTA solution (Sigma-Aldrich, St. Louis, USA) in PBS. Treatments with 1,25D, or compounds **2a-e** were carried out using medium supplemented with charcoal-treated FCS to remove liposoluble hormones. Control cells were treated with ethanol as vehicle.

Cell proliferation analyses. Two-dimensional (2D) cell proliferation was carried out in MCF-7, PC3, SKOV-3 and HaCaT cells using 3-(4,5-dimethylthiazol-2-yl)-2,5-diphenyltetrazolium bromide (MTT) assay as previously described.[46] Cells were treated with 1,25D or compounds **2a-e** at 10^{-8} or 10^{-7} M for 48 hours. Three-dimensional (3D) cell cultures were performed as previously described. Cells were then treated with 10^{-7} M of 1,25D and **2a-e** for 5 days. Phase contrast photographs three-dimensional cultures were taken with a Olympus DP72 camera. Quantitation of the sphere diameters was performed manually by tracing a straight line across the diameter of the sphere and scoring its value as relative units. Three-dimensional Cancer Stem Cell culture (3D-CSC) was performed using a commercial assay Cell2Sphere™ (Stemtek Therapeutics, Bilbao, Spain) containing the human breast adenocarcinoma MDA-MB-436 cell line enriched with CSCs under manufacturer's instructions. Ethanol (as control) or compound **2a** (10^{-8} or 10^{-7} M) were added for 5 days and quantitation of sphere number and diameter was performed as described above.

Human VDR Binding Assay. Binding affinity to VDR was evaluated using a 1,25D assay kit under manufacturer conditions (Polarscreen Vitamin D receptor competitor assay, Invitrogen) as previously described.[19] All **2a-e** compounds were evaluated within the range from 10^{-11} to 10^{-5} M. IC_{50} values were calculated using average of measured values. Activity of each compound is also shown as percentage, in which the activity of the 1,25D natural hormone was normalized to 100%.

Luciferase Reporter Assays. Luciferase reporter assays were performed as previously described.[19] Transfections were performed using 1 μg of pCYP24A1-Luc plasmid (kindly provided by Dr. Aranda). This vector encoding the luciferase gene under control of a consensus vitamin D response element (24-hydroxylase promoter, CYP24A1). After incubation for 24 h the medium was replaced by each compound (1,25D or **2a-e**) at concentrations 10^{-11} to 10^{-6} M. Bioluminescence images was acquired with the In Vivo Imaging System (IVIS, Caliper Life Sciences, Alameda, USA), and total photon counts were quantified using Living Image software (Caliper Life Sciences). The EC_{50} values are derived from dose-response curves and represent the analogue concentration capable of increasing the luciferase activity by 50%. The luciferase activity ratio is the average ratio of the EC_{50} for the analogue to the 1,25D value at the same dose.

Crystallization and Structure Determination. cDNA encoding zVDR LBD (156-453 AA) was cloned into pET28b vector to generate *N*-terminal His-tag fusion proteins. Purification was carried out as previously described, including metal affinity chromatography and gel filtration.[47] The protein was concentrated using Amicon ultra-30 (Millipore) to 3-7 mg/ml and incubated with a two-fold excess of ligand and a three-fold excess of the coactivator SRC-2 peptide (686-KHKILHRLLQDSS-698). Crystals were obtained in 50 mM Bis-Tris pH 6.5, 1.6 M lithium

sulfate and 50 mM magnesium sulfate. Protein crystals were mounted in a fiber loop and flash-cooled under a nitrogen flux after cryo-protection with 20% glycerol. Data collection from a single frozen crystal was performed at 100 K on the PX1 beamline at SOLEIL (France). The raw data were processed and scaled with the HKL2000 program suite.[48] The crystals belong to the space group $P6_522$, with one LBD complex per asymmetric unit. The structure was solved and refined using BUSTER,[49] Phenix[50] and iterative model building using COOT.[51] Crystallographic refinement statistics are presented in Table S2. All structural figures were prepared using PyMOL (www.pymol.org/).

Synthesis. General procedures and spectroscopic data (^{1}H, ^{13}C-NMR, HRMS, IR, [α]) for all compounds are described detailed in supporting information.

*Ethyl 6-(3-formylphenyl)hexanoate (**5**).* Aldehyde **3** (1.5 g, 8.1 mmol, 1 equiv) was dissolved in THF (5 mL). $Pd_2(dba)_3$ (0.074 g, 0.08 mmol, 0.01 equiv) and *t*Bu_3P (0.160 mL, 0.160 mmol, 0.02 equiv, 1M) were successively added. A solution of the organozinc compound **4**[30] (see supporting information) in THF (~1.5 equiv) was added and the reaction mixture was stirred at 23 ºC for 30 min. The reaction was quenched with saturated NH_4Cl (10 mL). The mixture was extracted with Et_2O (3x20 mL). The combined organic fractions were dried, filtered and concentrated in vacuo. The residue was purified by flash chromatography (2% EtOAc/hexanes) to afford ester **5** [1.95 g, 7.86 mmol, 97%, R_f = 0.45 (20% EtOAc/hexanes), colorless oil].

*Ethyl 6-[3-(2,2-dibromovinyl)phenyl] hexanoate (**6**).* A mixture of Ph_3P (3.96 g, 15.1 mmol, 2.5 equiv) and Zn (0.987 g, 15.1 mmol, 2.5 equiv) in CH_2Cl_2 (40 mL) was stirred at 23 ºC for 15 min and then cooled to 0 ^{o}C. After 5 min, CBr_4 (5 g, 15.1 mmol, 2.5 equiv) was added. The

reaction mixture was stirred at 0 ^{o}C for 1 h and at 23 ºC for 1.5 h. A solution of **5** (1.5 g, 6.04 mmol, 1 equiv) in CH_2Cl_2 (10 mL) was added *via* cannula. The mixture was stirred at 23 ºC for 1 h and filtered through a pad of celite (the solids were washed with Et_2O). The combined organic layers were concentrated in vacuo and the residue was purified by flash chromatography (2% EtOAc/hexanes) to afford dibromide **6** [2.24 g, 5.54 mmol, 92%, R_f = 0.68 (20% EtOAc/hexanes), brown oil].

*7-(3-Ethynylphenyl)-2-methylheptan-2-ol (**7**).* A solution of MeLi in Et_2O (19.8 mL, 29.7 mmol, 6 equiv, 1.5M) was added to a -78 ºC cooled solution of **6** (2 g, 4.95 mmol, 1 equiv) in THF (30 mL). The reaction mixture was allowed to reach 23 ºC. The reaction was quenched with sat NH_4Cl (20 mL). The mixture was extracted with Et_2O (3x20 mL). The combined organic fractions were dried, filtered and concentrated in vacuo. The residue was purified by flash chromatography (5% EtOAc/hexanes) to afford the alkyne **7a** [0.89 g, 3.86 mmol, 78%, R_f=0.3 (20% EtOAc/hexanes), colorless oil].

*7-(3-Ethynylphenyl)-2-methylheptan-2-triethylsilyl ether (**8**).* TESOTf (2.34 mL, 10.33 mmol, 1.5 equiv) and dry Et_3N (2.86 mL, 20.66 mmol, 3 equiv) were successively added to a -78 ºC cooled solution of compound **7** (1.58 g, 6.89 mmol, 1 equiv) in CH_2Cl_2 (30 mL). The mixture was stirred for 3 h. The reaction was quenched with sat NH_4Cl (20 mL). The mixture was extracted with Et_2O (3x30 mL). The combined organic fractions were dried, filtered and concentrated in vacuo. The residue was purified by flash chromatography (hexanes) to afford alkyne **8** [2.25 g, 6.53 mmol, 95%, R_f = 0.4 (1% EtOAc/hexanes), colorless oil].

*(E)-2-Methyl-7-{3-[1-(trimethylsilyl)but-1-en-2-yl]phenyl}heptan-2-triethylsilyl ether (**9a**).* A mixture of anhydrous LiCl (0.177 g, 4.18 mmol, 4.8 equiv) and CuI (0.206 g, 2.08 mmol, 2.4 equiv) was dried in a reaction tube at 120 ^{o}C for 3 h under vacuum. The mixture was allowed

to reach 23 ºC. THF (3 mL) was added and the resulting mixture was stirred at 23 ºC for 30 min. The homogeneous mixture was cooled to -60 ^{o}C and stirred for 5 min. A solution of EtMgBr in THF (1.4 mL, 4.18 mmol, 4.8 equiv, 3M) was added dropwise and the mixture was stirred at -60 ^{o}C for 1 h. Then, a solution of alkyne **8** (0.3 g, 0.87 mmol, 1 equiv) and HMPA (0.7 mL) in THF (5 mL) was added *via* cannula. After 5 min, a mixture of HMPA (0.3 mL) and freshly distilled TMSCl (0.53 mL, 4.18 mmol, 4.8 equiv) were successively added. The reaction mixture was allowed to reach 23 ºC for 7 h and then poured into sat NH_4Cl (15 mL). The solution was extracted with Et_2O (4x20 mL). The combined organic fractions were dried, filtered and concentrated in vacuo. The residue was purified by flash chromatography (hexanes) to afford vinylsilane **9a** [0.309 g, 0.69 mmol, 79%, R_f = 0.7 (1% EtOAc/hexanes), colorless oil].

(E)-7-[3-(1-Iodobut-1-en-2-yl)phenyl]-2-methylheptan-2-triethylsilyl ether (**10a**). *N*-Iodosuccinimide (0.151 g, 0.67 mmol, 1 equiv) was added to a -45 ºC cooled solution of vinylsilane **9a** (0.3 g, 0.67 mmol, 1 equiv) in CH_2Cl_2 (20 mL).The mixture was stirred for 3 h. The reaction was quenched with sat $Na_2S_2O_3$ (20 mL). The mixture was allowed to reach 23 ºC and extracted with CH_2Cl_2 (3x15 mL). The combined organic layers were dried, filtered and concentrated in vacuo. The residue was purified by flash chromatography (hexanes) to afford vinyl iodide **10a** [0.331 g, 0.66 mmol, 99%, R_f = 0.7 (1% EtOAc/hexanes), light yellow oil].

(E)-2-Methyl-7-{3-[1-(4,4,5,5-tetramethyl-1,3,2-dioxaborolan-2-yl]but-1-en-2-yl}phenyl)heptan-2-triethylsilyl ether (**11a**). $PdCl_2(dppf)\cdot CH_2Cl_2$ (0.0155 g, 0.019 mmol, 0.03 equiv), KOAc (0.188 g, 1.92 mmol, 3 equiv, dried in *vacuo* at 120 ^{o}C for 2 h) and bis(pinacolato)diboron (0.195 g, 0.77 mmol, 1.2 equiv) were successively added to a solution of vinyl iodide **10a** (0.32 g, 0.64 mmol, 1 equiv) in DMSO (3 mL). The reaction mixture was stirred at 80 ^{o}C for 1 h

and then allowed to reach 23 ºC. Water (10 mL) was added and the mixture was extracted with Et_2O (3x10 mL). The combined organic fractions were dried, filtered and concentrated in vacuo. The residue was purified by flash chromatography (1% EtOAc/hexanes) to afford vinyl boronic ester **11a** [0.227 g, 0.45 mmol, 71%, R_f = 0.57 (3% EtOAc/hexanes), light brown oil].

(1R,3S,Z)-5-{(E)-3-[3-(6-Hydroxy-6-methylheptyl)phenyl]pent-2-en-1-ylidene}-4-methylenecyclohexane-1,3-diol (**2a**). Aqueous K_3PO_4 (3 mL, 2M) and $PdCl_2(PPh_3)_2$ (0.007 g, 0.01 mmol, 0.05 equiv) were successively added to a solution of boronate **11a** (0.1 g, 0.2 mmol, 1 equiv) and enol-triflate **12** (0.14 g, 0.233 mmol, 1.17 equiv) in THF (10 mL). The reaction mixture was vigorously stirred at 23 ºC for 1.5 h and then diluted with H_2O (5 mL). The mixture was extracted with Et_2O (3x10 mL). The combined organic layers were dried, filtered and concentrated in vacuo. The residue was purified by flash chromatography (1% Et_2O/hexanes) to afford the protected compound which was dissolved in THF (5 mL). A solution of TBAF in THF (1.2 mL, 1.2 mmol, 6 equiv, 1M) was added. The mixture was stirred at 23 ºC for 24 h and then diluted with sat NH_4Cl (5 mL). The mixture was extracted with EtOAc (5x10 mL). The combined organic layers were dried, filtered and concentrated in vacuo. The residue was purified by flash chromatography (70% EtOAc/hexanes) to afford **2a** [0.053 g, 0.133 mmol, 67%, R_f = 0.4 (90% EtOAc/hexanes), colorless oil], which was further purified by HPLC (22% *i*PrOH/hexanes). $[\alpha]_D^{25}$= +19.1^o (*c* = 1.2 in EtOH).

ASSOCIATED CONTENT

Accession Code. The atomic coordinates and structure factors have been deposited in the Protein Data Bank, Research Collaboratory for Structural Bioinformatics, Rutgers University, New

Brunswick, New Jersey, with entry code 6FOD (compound **2a**), 6FO9 (compound **2b**), 6FO7 (compound **2c**), 6FO8 (compound **2d**) and 6FOB (compound **2e**). Authors will release the atomic coordinates and experimental data upon article publication.

Supporting Information. The Supporting Information is available free of charge on the ACS Publications website at DOI: 10.1021/acs.jmedchem.xxxx.

Additional supplemental figures, synthetic procedures and characterization data for compounds along with protocols for cell culture, MTT metabolization, human VDR binding affinity, luciferase reporter assays, Western blot assays and animal studies, crystallization assays and refinement of the crystals can be found in SI appendix. Each analog reported as a novel compound in this study (**2a**, **2b**, **2c**, **2d** and **2e**) present a single sharp peaks on HPLC (Phenomenex Luna 5μ Silica(2) 100A, 250 x 21.2 mm, normal phase; isocratic mode; *i*PrOH/hexanes). HPLC analysis was used to determine the purity (>95%) of the vitamin D analogues.

AUTHOR INFORMATION

Corresponding Authors

* E-mail: roman.perez.fernandez@usc.es

* E-mail: rochel@igbmc.fr

* E-mail: antonio.mourino@usc.es

Author Contributions

P.G., S.S., R.S., T.G., N.R. conducted experiments; M.A.M, R.P.F., N.R., A.M. designed experiments; all authors contributed to the writing of the paper.

# These authors contributed equally.

Notes

The authors declare no competing financial interest.

ACKNOWLEDGMENTS

We thank the Spanish Ministry of Science and Innovation (SAF2010-15291, FEDER to AM), Ministry of Economy and Competitiveness (SAF2015-69221-R, MINECO/FEDER to RP-F), and Xunta de Galicia (GPC2014/001). The work was also supported by grant ANR-13-BSV8-0024-01 (N.R.) from ANR and institutional funds (N.R.) from Instruct-ERIC for support and the use of resources of the French Infrastructure for Integrated Structural Biology. We thank CESGA for the computing time. RS thanks Xunta de Galicia for a Postdoctoral Fellowship (Plan I2C ano 2012, modalidade A). The authors would like to thank the staff of Proxima 1 at SOLEIL for assistance in using the beamlines and Alastair McEwen (IGBMC) for help in X-ray data collections.

ABBREVIATIONS

1,25D, 1α,25-dihydroxyvitaminD_3; VDR, vitamin D receptor; LBD, ligand binding domain.

REFERENCES

1 Plum, L. A.; DeLuca, H. F. Vitamin D, disease and therapeutic opportunities. *Nat. Rev. Drug Discovery* **2010**, *9*, 941-955.

2 Leyssens, C.; Verlinden, L.; Verstuyf, A. The future of vitamin D analogs. *Front. Physiol.* **2014**, *5*, 1-18.

3 Binderup, L.; Binderup, E.; Godfredsen, W. O. Development of new vitamin D analogs. In *Vitamin D*; Feldman, D., Glorieux, F. H., Pike, J. W., Eds.; Academic Press: San Diego, CA, 1997; Vol.*61*, pp 1027-1041.

4 Kubodera, N.; Sato, K.; Nishii, Y. Characteristics of 22-oxacalcitriol (OCT) and 2β-(3-hydroxypropoxy)-calcitriol (ED-71). In *Vitamin D*; Feldman, D., Glorieux, F. H., Pike, J. W., Eds.; Academic Press: San Diego, CA, 1997; Vol.*61*, pp 1071-1086.

5 G. Jones. Analog metabolism. In *Vitamin D*; Feldman, D., Glorieux, F. H., Pike, J. W., Eds.; Academic Press: San Diego, CA, 1997; Vol. *61*, pp 973-994.

6 Slatopolsky, E.; Finch, J.; Ritter, C.; Denda, M.; Morrissey, J.; Brown, A.; DeLuca, H. F. A new analog of calcitriol, 19-nor-1,25-$(OH)_2D_2$, suppresses parathyroid hormone secretion in uremic rats in the absence of hypercalcemia. *Am. J. Kidney Dis.* **1995**, *26*, 852-860.

7 Uskokovic, M. R.; Studzinski, G. P.; Reddy, G. S. The 16-ene vitamin D analogs. *Vitamin D*, eds Feldman D, Glorieux FH, Pike JW (Academic, New York), 1997, *62*, 1045.

8 Kensler, T. W.; Dolan, P. M.; Gange, S. J.; Lee, J. K.; X Wang, Q.; Posner, G. H. Conceptually new deltanoids (vitamin D analogs) inhibit skin tumorigenesis. *Carcinogenesis* **2000***, 21*, 1341-1345.

9 Verlinden, L.; Verstuyf, A.; Van Camp, M.; Marcelis, S.; Sabbe, K.; Zhao, X. Y.; De Clercq, P.; Vandewalle, M.; Bouillon, R. Two novel 14-epi-analogues of 1,25-dihydroxyvitamin D_3 inhibit the growth of human breast cancer cells in vitro and in vivo. *Cancer Res*. **2000**, *60*, 2673-2679.

10 Ma, Y.; Yu, W. D.; Hidalgo, A. A. ; Luo, W.; Delansorne, R.; Johnson, C. S.; Trump, D. L. Inecalcitol, an analog of $1,25D_3$ displays enhanced antitumor activity through the induction of apopotosis in a squamous cell carcinoma model system. *Cell Cycle* **2013**, *12*, 743-752.

11 Molnar, F.; Sigüeiro, R.; Sato, Y.; Araujo, C.; Schuste, I.; Antony, P.; Peluso, J.; Muller, C.; Mouriño, A.; Moras, D.; Rochel, N. 1α,25(OH)$_2$-epi-vitamin D$_3$, a natural physiological metabolite of vitamin D$_3$: its synthesis, biological activity and crystal structure with its receptor. *PLoS ONE*, **2011**, *6,* e18124.

12 Plum, L. A.; Prahl, J. M.; Ma, X.; Sicinski, R. R.; Gowlugari, S.; Clagett-Dame, M.; DeLuca, H. F. Biologically active noncalcemic analogs of 1α,25-dihydroxyvitamin D with an abbreviated side chain containing no hydroxyl. *Proc. Natl. Acad. Sci. USA,* **2004**, *101*, 6900-6904.

13 Otero, R.; Seoane, S.; Sigüeiro, R.; Belorusova, A. Y.; Maestro, M. A.; Pérez-Fernández, R.; Rochel, N.; Mouriño, A. Carborane-based design of a potente vitamin D receptor agonist. *Chem. Sci.* **2016**, *7*, 1033-1037.

14 Yamada, S.; Makishima, M. Structure-activity relationship of nonsecosteroidal vitamin D receptor modulators. *Trends Pharmacol. Sci.* **2014***, 35*, 324-337.

15 Ma, Y.; Khalifa, B.; Yee, Y. K.; Lu, J.; Memezawa, A.; Savkur, R. S.; Yamamoto, Y.; Chintalacharuvu, R. S.; Yamaoka, K.; Stayrook, K. R.; Bramlett, K. S.; Zeng, Q. Q.;Chandrasekhar, S.; Yu, X. P.; Linebarger, J. H.; Iturria, S. J.; Burris, T. P.; Kato, S.; Chin, W. W.; Nagpal, S. Identification and characterization of noncalcemic, tissue-selective, nonsecosteroidal vitamin D receptor modulators. *J. Clin. Invest.* **2006**, *116*, 892-904.

16 Gogoi, P.; Sigüeiro, R.; Eduardo, S; Mouriño, A. An expeditious route to 1α,25-dihydroxyvitamin D$_3$ and its analogues by an aqueous tandem palladium-catalyzed A-ring closure and Suzuki coupling to the C/D unit. *Chem. Eur. J.* **2010**, *16*, 1432-1435.

17 López-Pérez, B.; Maestro, M. A.; Mouriño, A. Total synthesis of 1α,25-dihydroxyvitamin D$_3$ (calcitriol) through a Si-assisted allylic substitution. *Chem. Comm.* **2017**, *53*, 8144-8147.

18 Sokolowska, S.; Carballa, D.; Seoane, S.; Pérez-Fernández, R.; Mouriño, A.; Sicinski, R. R. Synthesis and biological activity of two C-7 methyl analogues of vitamin D. *J. Org. Chem.* **2015**, *80*, 165-173.

19 Carballa, D. M.; Seoane, S.; Zacconi, F.; Pérez, X.; Rumbo, A., Alvarez-Díaz, S.; Larriba, M. J.; Pérez-Fernández, R.; Muñoz, A.; Maestro, M.; Mouriño, A.; Torneiro, M. Synthesis and biological evaluation of 1α,25-dihydroxyvitamin D_3 analogues with a long side chain at C12 and short C17 side chains. *J. Med. Chem.* **2012***, 55*, 8642-8656.

20 Antony, P.; Sigüeiro, R.; Huet, T.; Sato, Y.; Ramalanjaona, N.; Rodrigues, L. C.; Mouriño, A.; Moras, D.; Rochel, N. Structure-function relationships and crystal structures of the vitamin D receptor bound 2α-methyl-(20*S*,23*S*)- and 2α-methyl-(20*S*,23*R*)-epoxymethano-1α,25-dihydroxyvitamin D_3. *J. Med. Chem.* **2010***, 53*, 1159-1171.

21 Zhu, G. D.; Chen, Y. J.; Zhou, X. M.; Vandewalle, M.; De Clercq, P. J. Synthesis of CD-ring modified 1α,25-dihydroxy vitamin D analogues: C-ring analogues. *Bioorg. Med. Chem. Lett.* **1996**, *6*, 1703-1708.

22 Zhou, X. M.; Zhu, G. D.; Van Haver, D.; Vandewalle, M.; De Clercq, P. J.; Verstuyf, A.; Bouillon, R. Synthesis, biological activity, and conformational analysis of four *seco*-D-15,19-*bisnor*-1α,25-dihydroxyvitamin D analogues, diastereomeric at C17 and C20. *J. Med. Chem.* **1999***, 42*, 3539-3556.

23 Verstuyf, A.; Verlinden, L.; Van Etten, E.; Shi, L.; Wu, Y.; D'Halleweyn, C.; Van Haver, D.; Zhu, G. D.; Chen, Y. J.; Zhou, X.; Haussler, M. R.; De Clercq, P.; Vandewalle, M.; Van Baelen, H.; Mathieu, C.; Bouillon, R. Biological activity of CD-ring modified 1α,25-dihydroxyvitamin D analogues: C-ring and five-membered D-ring analogues. *J. Bone Min. Res.* **2000**, *15*, 237-252.

24 Yong, W.; Ling, S.; D'Halleweyn, C.; Van Haver, D.; De Clercq, P.; Vandewalle, M.; Bouillon, R.; Verstuyf, A. Synthesis of CD-ring modified 1α,25-dihydroxy vitamin D analogues: five-membered D-ring analogues. *Bioorg. Med. Chem. Lett.* **1977**, *7*, 923-928.

25 Linclau, B.; De Clercq, P.; Vandewalle, M.; Bouillon, R.; Verstuyf, A. The Synthesis of CD-ring modified 1α,25-dihydroxy vitamin D analogues: Six-membered D-ring analogues I. *Bioorg. Med. Chem. Lett.,* **1977**, *7*, 1461-1464.

26 Vrielynck, F.; Van Haver, D.; Vandewalle, M.; Verlinden, L.;Verstuyf, A.; Bouillon, R.; Croce, G.; DeClercq, P. Development of analogues of 1α,25-dihydroxyvitamin D3 with biased side-chain orientation: C20 methylated des-C,D-homo analogues. *Eur. J. Org. Chem.* **2009**, 1720-1737.

27 Eelen, G.; Verlinden, L.; Bouillon, R.; De Clercq, P.; Muñoz, A.; Verstuyf, A. CD-ring modified vitamin D_3 analogs and their superagonistic action. *J. Steroid. Biochem. Mol. Biol.* **2010**, *121,* 417-419.

28 Hourai, S.; Rodrigues, L. C.; Antony, P.; Reina-San-Martin, B.; Ciesielski, F.; Magnier, B. C.; Schoonjans, K.; Mouriño, A.; Rochel, N.; Moras, D. Structure-based design of a superagonist ligandfor the vitamin D nuclear receptor. *Chem. Biol*. **2008**, *15*, 383-392.

29 Rochel, N.; Wurtz, J. M.; Mitschler, A.; Klaholz, B.; Moras, D. The crystal structure of the nuclear receptor for vitamin D bound to its natural ligand. *Mol. Cell* **2000***, 5*, 173-179.

30 Krasovskiy, A.; Malakhov, V.; Gavryushin, A.; Knochel, P. Efficient synthesis of functionalized organozinc compounds by the direct insertion of zinc into organic iodides and bromides. *Angew Chem. Int. Ed.* **2006**, *45*, 6040-6044

31 Corey, E. J.; Fuchs, P. L. A synthetic method for formyl→ethynyl conversion (RCHO→RC≡CH or RC≡CR′). *Tetrahedron Lett.* **1972**, *13*, 3769-3772.

32 Ishiyama, T.; Murata, T.; Miyaura, M. Palladium(0)-catalyzed cross-coupling reaction of alkoxydiboron with haloarenes: a direct procedure for arylboronic esters. *J. Org. Chem.* **1995***, 60*, 7508-7510.

33 Deeb, K. K.; Trump D. L.; Johnson, C. S. Vitamin D signalling pathways in cancer: potential for anticancer therapeutics. *Nat. Rev. Cancer* **2007***, 7,* 684-700.

34 Feldman, D.; Krishnan, A. V.; Swami, S.; Giovannucci, E.; Feldman, B. J. The role of vitamin D in reducing cancer risk and progression. *Nat. Rev. Cancer* **2014**, *14*, 342-357.

35 Ma, Y.; Trump D. L.; Johnson, C. S. Vitamin D in combination cancer treatment. *J. Cancer* **2010**, *1*: 101-107.

36 Buras, R. R.; Schumaker, L. M.; Davood, F.; Brenner, R. V.; Shabahang, M.; Nauta, R. J.; Evans, S. R. Vitamin D receptors in breast cancer cells. *Breast Cancer Res. Treat.* **1994***, 31*, 191-202.

37 Santagata, S.; Thakkar, A.; Ergonul, A.; Wang, B.; Woo, T.; Hu, R.; Harrell, J. C.; McNamara, G.; Schwede, M.; Culhane, A. C.; Kindelberger, D.; Rodig, S.; Richardson, A.; Schnitt, S. J.; Tamimi, R. M.; Ince, T. A. Taxonomy of breast cancer based on normal cell phenotype predicts outcome. *J. Clin. Invest.* **2014**, *124*, 859-870.

38 Liu, S.; Dontu, G.; Wicha, M. S. Mammary stem cells, self-renewal pathways, and carcinogenesis. *Breast Cancer Re*s. **2005**, *7*, 86-95.

39 Yang, F.; Xu, J.; Tang, L.; Guan, X. Breast cancer stem cell: the roles and therapeutic implications. *Cell Mol. Life Sci.* **2017***, 74*, 951-966.

40 Belorusova, A. Y.; Rochel, N. Structural studies of vitamin D nuclear receptor ligand-binding properties. *Vitam. Horm.* **2016**, *100*, 83-116.

41 Eelen, G.; Verlinden, L.; Bouillon, R.; De Clercq, P.; Muñoz, A.; Verstuyf, A. CD-ring modified vitamin D_3 analogs and their superagonistic action. *J. Steroid. Biochem. Mol. Biol.* **2010**, *121,* 417-419.

42 Eelen, G., Verlinden, L., Rochel, N., Claessens, F., De Clercq, P., Vandewalle, M., Tocchini-Valentini, G., Moras, D., Bouillon, R., Verstuyf, A. Superagonistic action of 14-epi-analogs of 1,25-dihydroxyvitamin D explained by vitamin D receptor-coactivator interaction. *Mol Pharmacol.* **2005**, *67*, 1566-1573.

43 Ciesielski, F.; Sato, Y.; Chebaro, Y.; Moras, D.; Dejaegere, A.; Rochel, N. Structural basis for the accommodation of bis- and tris-aromatic derivatives in vitamin D nuclear receptor. *J. Med. Chem.* **2012**, *55*, 8440-8849.

44 InsightII, Discover and Builder are trademarked software of Accelrys Inc., San Diego, CA

45 Dauber-Osguthorpe, P.; Roberts, V. A.; Osguthorpe, D. J.; Wolff, J.; Genest, M.; Hagler, A. T. Structure and energetics of ligand binding to proteins: *E. coli* dihydrofolate reductase-trimethoprim, a drug-receptor system. *Proteins: Structure, Function and Genetics* **1998**, *4*, 31-47.

46 Seoane, S.; Arias, E.; Sigüeiro, R.; Sendon-Lago, J.; Martínez-Ordóñez, A.; Castelao, E.; Eiró, N; García-Caballero, T.; Macías, M.; López-López, R.; Maestro, M.; Vizoso, F.; Mouriño, A.; Pérez-Fernández, R. Pit-1 inhibits BRCA1 and sensitizes human breast tumors to cisplatin and vitamin D treatment. *Oncotarget* **2015**, *6*, 14456-14471.

47 Belorusova, A. Y.; Eberhardt, J.; Potier, N.; Stote, R. H.; Dejaegere, A.; Rochel, N. Structural insights into the molecular mechanism of vitamin D receptor activation by

lithocholic acid involving a new mode of ligand recognition. *J. Med. Chem*. **2014**, *57*, 4710-4719.

48 Otwinowski, Z.; Minor, W. Processing of X-ray diffraction data collected in oscillation mode. *Method Enzymol.* **1997**, *276*, 307-326.

49 Bricogne, G.; Blanc, E.; Brandl, M.; Flensburg, C.; Keller, P.; Paciorek, W.; Roversi, P.; Sharff, A; Smart, O. S.; Vonrhein, C.; Womack, T. O. BUSTER version 2.11.2. Cambridge, United Kingdom: Global Phasing Ltd 2011.

50 Adams, P. D.; Afonine, P. V.; Bunkoczi, G.; Chen, V. B.; Davis, I. W.; Echols, N.; Headd, J. J.; Hung, L. W.; Kapral, G. J.; Grosse-Kunstleve, R. W.; McCoy, A. J., Moriarty, N. W.; Oeffner, R.; Read, R. J.; Richardson, D. C.; Richardson, J. S; Terwilliger, T. C; Zwart, P. H. PHENIX: a comprehensive Python-based system for macromolecular structure solution. *Acta Crystallogr. D* **2010**, *66*, 213-221.

51 Emsley, P.; Cowtan, K. Coot: model-building tools for molecular graphics. *Acta Crystallogr. D* **2004**, *60*, 2126-2132.

Figures Legend

Figure 1. Aromatic-based design of 1,25D analogs. (**a**) Structures of 1,25D and the analogs **2a**-**e**. (**b**) Superimposition of ligands **2** from docking analysis [**2a** (green), **2b** (blue), **2c** (pink), **2d** (yellow), **2e** (orange)] in the VDR Ligand Binding Pocket with 1,25D (white).

Scheme 1. Synthesis of the analogs **2a-e**.

Figure 2. Differentiation and Western blot of vitamin D targets. (**a**) Differentiation activity in human HaCaT keratinocyte cells treated with 100 nM of 1,25D and **2a-e** compounds for 48 hours. (**b**) MCF-7 cells were treated with 10^{-9} to 10^{-7} M of 1,25D and **2a-e** compounds for 48 hours and then a Western blot was carried out to evaluate p21, p27 and p53 expression. Expression values were obtained by densitometry analyses.

Figure 3. Biological effects of compound **2a. (a)** Calcemic activity in mice after 21 days of treatment every other day with vehicle, 1,25D and compound **2a**. **(b)** SCID mice were subcutaneously injected with MDA-MB-231-luc cells. Ten days later (day 0 of treatment), mice were split up into 2 groups and injected intraperitoneally (i.p.) with the compound **2a** (1µg/kg weight, dissolved in sesame oil). The control group was treated with vehicle (sesame oil). Tumor growth was monitored every 7 days from day 10 (0 day of treatment) until day 28 using *in Vivo* Imaging System. **(c)** Representative image of mice described in b. Panel in c indicates bioluminescence intensity (PF = Photon flux). **(d)** Animals were treated as described in (b) until day 60 to calculate overall survival. **(e)** Three-dimensional Cancer Stem Cell culture (3D-CSC) was performed in human breast adenocarcinoma MDAMB-436 cells enriched with CSCs and treated with ethanol or compound **2a** (10^{-8} or 10^{-7} M) for 5 days. Sphere growth and number of 3D cultures was quantified and represented in **(f)** and **(g)** Error bars represent standard deviation (SD).

Figure 4. X-ray crystal structures of zVDR LBD complexes with **2a-e**. (**a**) Superposition of **2a**, **2b**, **2c**, **2d** and **2e**. **(b)** Hydrogen bonds formed by **2a** are shown by red dotted lines. **(c)** Hydrogen bonds formed by **2b**. **(d)** Hydrogen bonds formed by **2c**. (**e**) Hydrogen bonds formed by **2d**. **(f)** Hydrogen bonds formed by **2e**. Ligands **2a-e** are superimposed with 1,25D (grey).

Figure 5. **(a)** Interactions of **2a** with VDR residues within 4 Å distance. Residues interacting with the **A**- and seco-**B**-rings are colored and labelled in cyan, residues interacting with the central part of the ligand are colored and labelled in green and those interacting with the terminal aliphatic side chain in grey. **(b)** Interactions of **2e** with VDR residues within 4 Å distance. Same color for the residues as in Figure 4a. **(c)** Overlay of the crystal structures of zVDR-**2a** and zVDR-**2e.** Residues interacting with the central part and terminal side chain of the compounds

are shown. The heptyl central group of **2e** induces some conformational changes of some side chains and a different positioning of the terminal side chain.

Table 1. Two- (2D) and three-(3D) dimensional cellular proliferation (expressed as percentage ± SD with respect to vehicle treated cells) of the human breast adenocarcinoma MCF-7, the human prostate adenocarcinoma PC-3, the human ovarian cancer SKOV-3, and the human keratinocyte HaCaT cell lines after culture for 48 h (2D) and 5 days (3D) with 100 nM of 1,25D and the **2a-2e** compounds. Transcriptional activity is expressed as EC_{50} molar range, and as percentage of the EC_{50} M mean with respect to 1,25D (100%). Serum calcium levels (mean ± SD) in mice treated every other day for 21 days with 1,25D and the **2a-2e** compounds (0.3 μg/kg weight, n=5 per group). VDR binding of the 1,25D and the **2a-2e** compounds expressed as IC_{50} M range, and as percentage of the IC_{50} M mean with respect to 1,25D.

FIGURES and SCHEMES

Figure 1

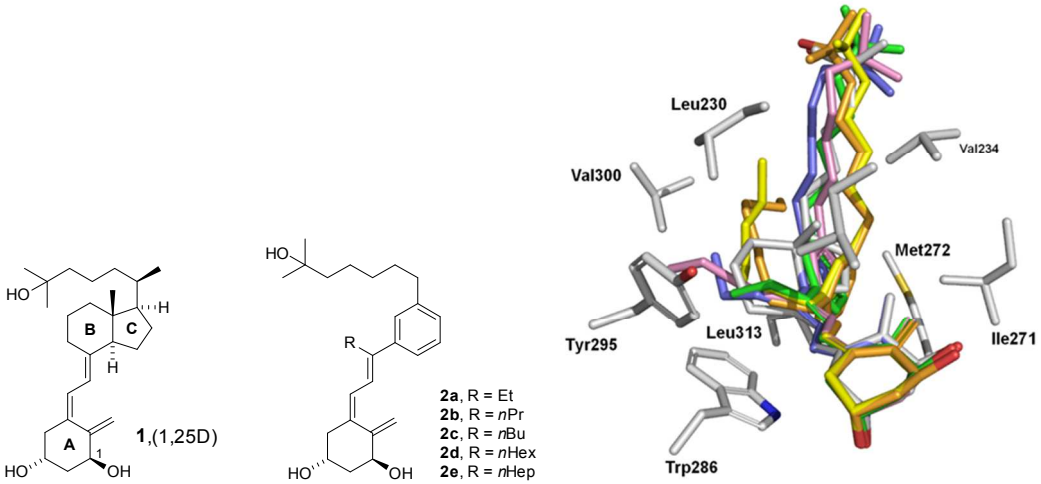

Scheme 1

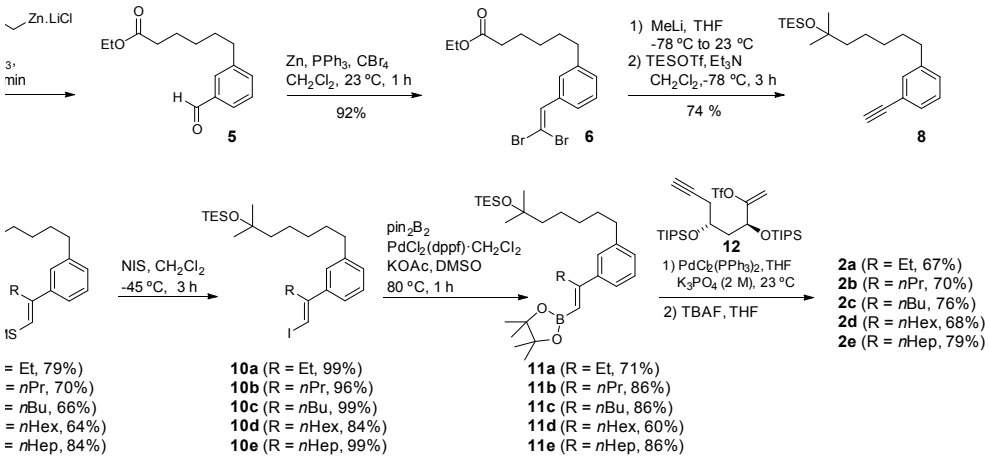

Figure 2

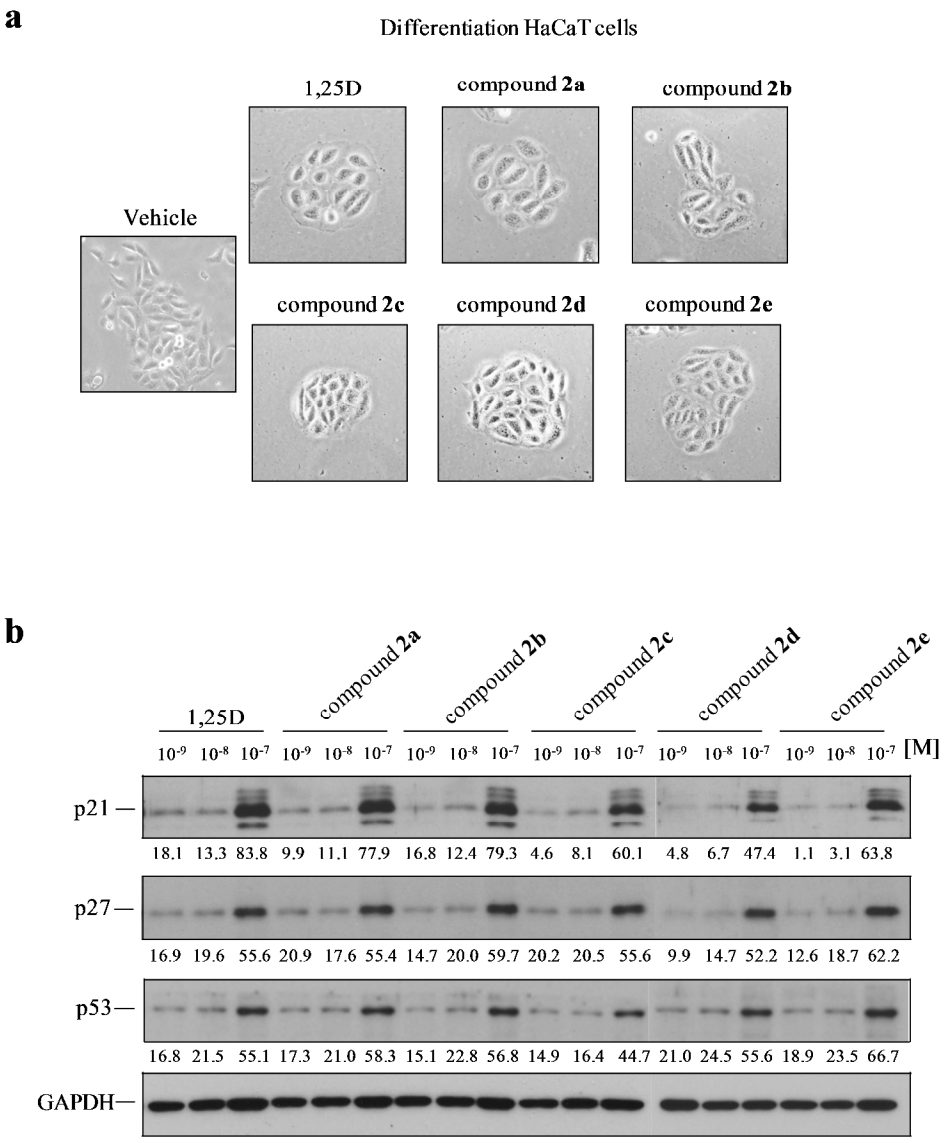
a
Differentiation HaCaT cells
Vehicle
1,25D
compound 2a
compound 2b
compound 2c
compound 2d
compound 2e
b
1,25D
compound 2a
compound 2b
compound 2c
compound 2d
compound 2e
10-9 10-8 10-7 [M]
p21
18.1 13.3 83.8 9.9 11.1 77.9 16.8 12.4 79.3 4.6 8.1 60.1 4.8 6.7 47.4 1.1 3.1 63.8
p27
16.9 19.6 55.6 20.9 17.6 55.4 14.7 20.0 59.7 20.2 20.5 55.6 9.9 14.7 52.2 12.6 18.7 62.2
p53
16.8 21.5 55.1 17.3 21.0 58.3 15.1 22.8 56.8 14.9 16.4 44.7 21.0 24.5 55.6 18.9 23.5 66.7
GAPDH

Figure 3.

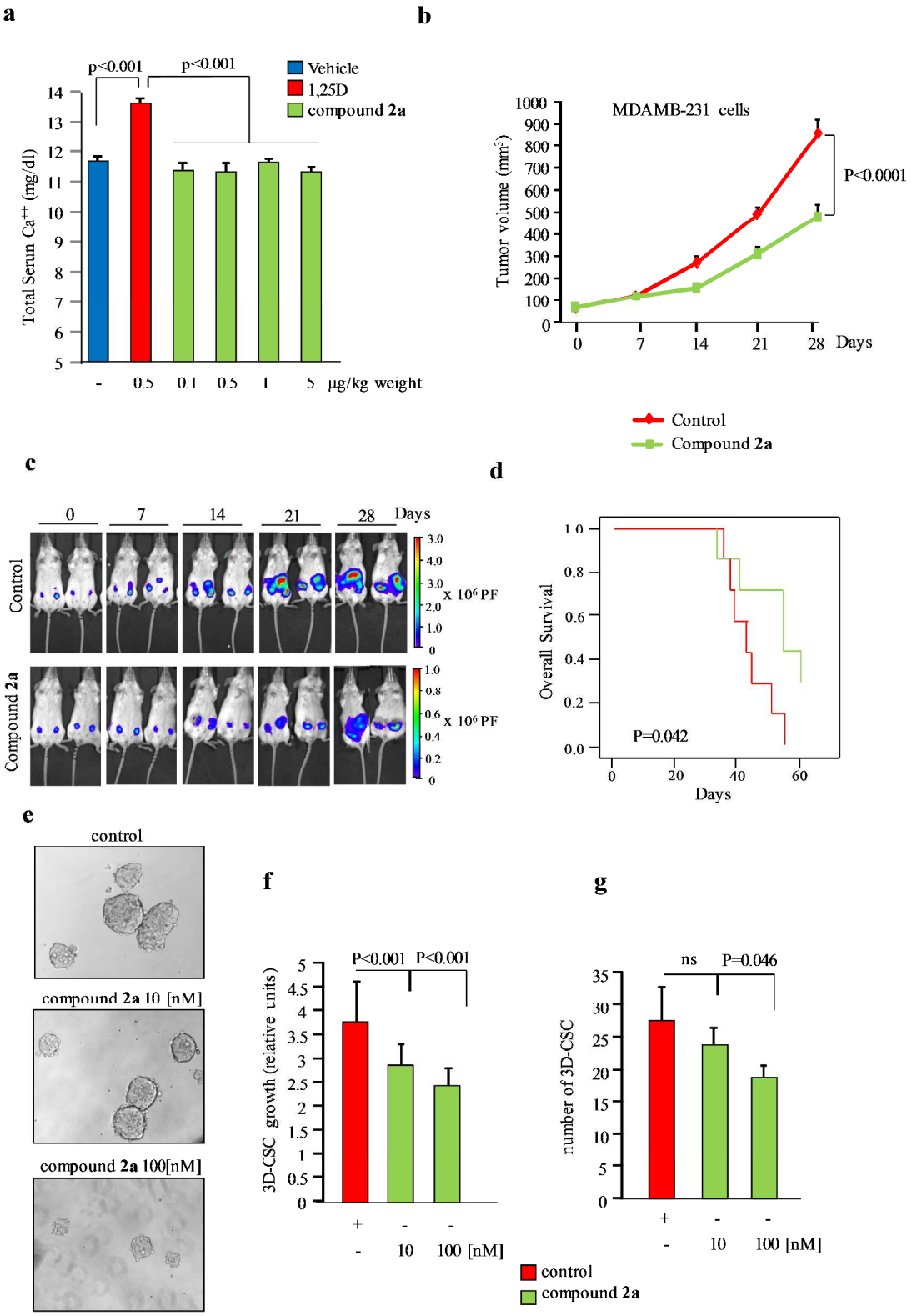
a
p<0.001
p<0.001
Vehicle
1,25D
compound 2a
Total Serun Ca++ (mg/dl)
14
13
12
11
10
9
8
7
6
5
-
0.5
0.1
0.5
1
5
µg/kg weight
b
MDAMB-231 cells
Tumor volume (mm3)
1000
900
800
700
600
500
400
300
200
100
0
P<0.0001
0
7
14
21
28
Days
Control
Compound 2a
c
0
7
14
21
28
Days
Control
Compound 2a
3.0
4.0
3.0
2.0
1.0
0
x 10⁶ PF
1.0
0.8
0.6
0.4
0.2
0
x 10⁶ PF
d
Overall Survival
1.0
0.8
0.6
0.4
0.2
0.0
P=0.042
0
20
40
60
Days
e
control
compound 2a 10 [nM]
compound 2a 100[nM]
f
P<0.001
P<0.001
3D-CSC growth (relative units)
5
4.5
4
3.5
3
2.5
2
1.5
1
0.5
0
+
-
-
-
10
100 [nM]
g
ns
P=0.046
number of 3D-CSC
35
30
25
20
15
10
5
0
+
-
-
-
10
100 [nM]
control
compound 2a

Figure 4.

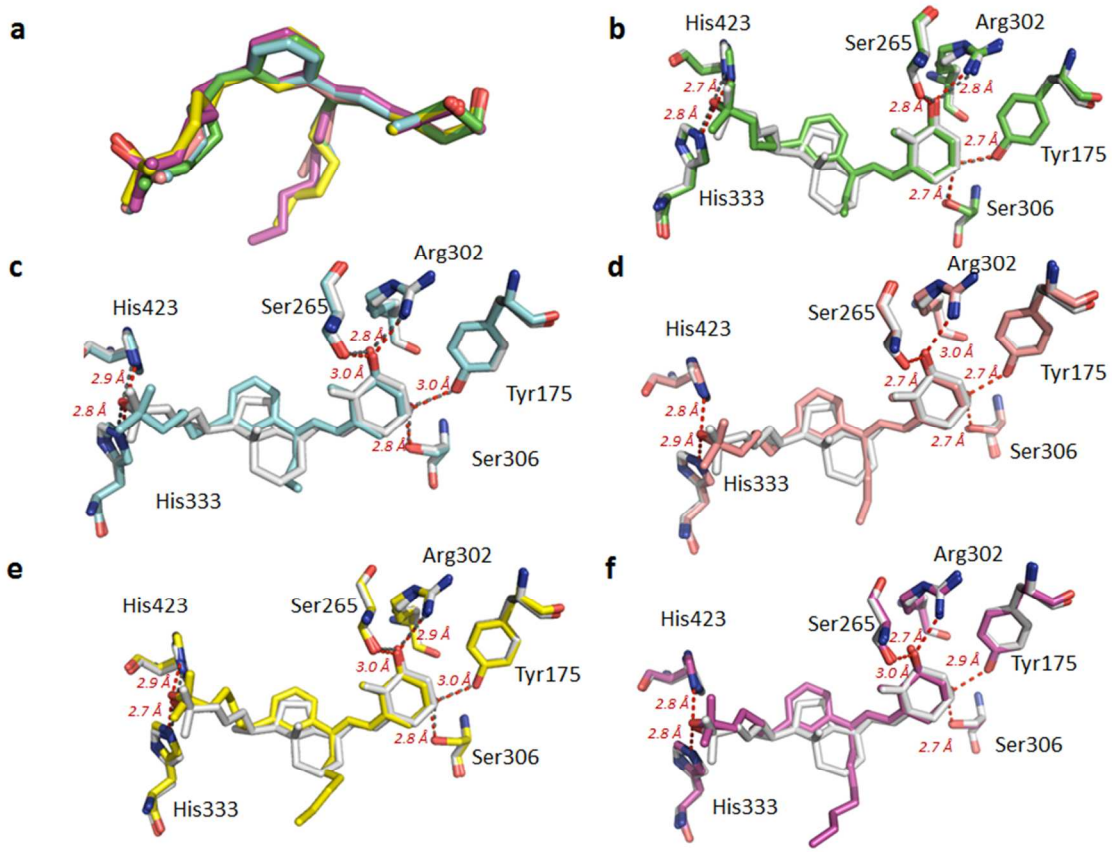
a
b
His423
Ser265
Arg302
2.7 Å
2.8 Å
2.8 Å
2.8 Å
2.7 Å
Tyr175
His333
2.7 Å
Ser306
c
Arg302
His423
Ser265
2.8 Å
2.9 Å
3.0 Å
3.0 Å
Tyr175
2.8 Å
2.8 Å
Ser306
His333
d
Arg302
Ser265
His423
3.0 Å
2.7 Å
2.7 Å
Tyr175
2.8 Å
2.9 Å
2.7 Å
Ser306
His333
e
Arg302
His423
Ser265
2.9 Å
3.0 Å
2.9 Å
3.0 Å
Tyr175
2.7 Å
2.8 Å
Ser306
His333
f
Arg302
His423
Ser265
2.7 Å
2.9 Å
3.0 Å
Tyr175
2.8 Å
2.8 Å
2.7 Å
Ser306
His333

Figure 5.

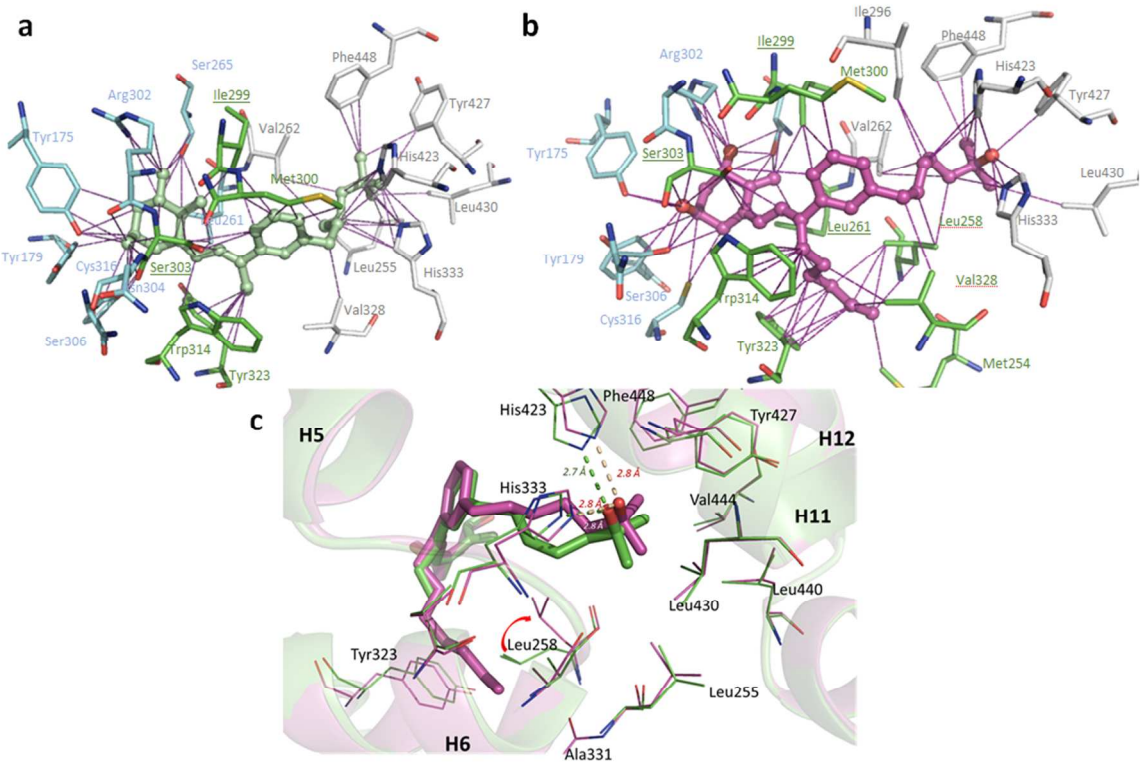
a
Ser265
Phe448
Arg302
Ile299
Tyr427
Val262
Tyr175
His423
Met300
Leu430
Leu261
Tyr179
Cys316
Ser303
Leu255
His333
Asn304
Val328
Ser306
Trp314
Tyr323
b
Ile296
Arg302
Ile299
Phe448
Met300
His423
Tyr427
Val262
Tyr175
Ser303
Leu430
Leu261
Leu258
His333
Tyr179
Val328
Ser306
Trp314
Cys316
Tyr323
Met254
c
H5
His423
Phe448
Tyr427
H12
2.7Å
2.8Å
His333
2.8Å
2.8Å
Val444
H11
Leu430
Leu440
Leu258
Tyr323
Leu255
H6
Ala331

Table 1.

	Cellular proliferation				Transcriptional activity	Calcemia	VDR binding
	MCF-7 (%)	PC-3 (%)	SKOV-3 (%)	HaCaT (%)			
	2D - 3D	2D	2D	2D	EC_{50} M range (%)	mg/dl (%)	IC_{50} M range (%)
1,25D	66±2.3 - 61±9.6	77±1.2	78±2.3	69±1.5	1.6 - $2.3x10^{-9}$ (100)	14.7±0.5 (100)	1.3 - $2.3x10^{-9}$ (100)
2a	65±2.4 - 69±10.3	78±2.4	78±3.4	68±1.1	5.6 - $6.2x10^{-9}$ (33)	11.8±1.4 (0)	$4.5x10^{-9}$ - $1.1x10^{-8}$ (24)
2b	69±2.8 - 74±10.3	83±3.0	82±2.9	71±1.3	8.6 - $9.9x10^{-9}$ (21)	13.1±1.2 (41)	$5.6x10^{-9}$ - $5.5x10^{-8}$ (10)
2c	74±2.4 - 84±8.2	84±5.6	81±5.3	71±1.0	$9.0x10^{-9}$ - $1.1x10^{-8}$ (19)	12.9±0.8 (34)	1.0 - $1.8x10^{-8}$ (12)
2d	78±2.9 - 79±7.5	80±1.9	76±0.9	74±2.1	1.0 - $1.3x10^{-8}$ (17)	11.7±0.8 (0)	$8.3x10^{-9}$ - $4.0x10^{-8}$ (9)
2e	69±4.4 - 55±6.2	79±3.2	83±5.6	71±3.2	2.9 - $4.0x10^{-8}$ (5)	10.9±1.3 (0)	$3.5x10^{-9}$ - $1.6x10^{-7}$ (7)